ACADEMIA ROMÂNĂ
Revue Roumaine de Chimie
http://web.icf.ro/rrch/

Rev. Roum. Chim.,
2017, *62*(3), 277-289

MS, CD, AND FT-IR CHARACTERIZATION OF FIVE NEWLY SYNTHESIZED HISTIDINE-CONTAINING Ala- AND Gly-BASED PEPTIDES

Manuela MURARIU,[a] Laura ION,[b] Catalina-Ionica CIOBANU,[c]
Brindusa Alina PETRE[b] and Gabi DROCHIOIU [a,b,*]

[a] "Petru Poni" Institute of Macromolecular Chemistry, 41a Ghica Voda Alley, Iaşi-700487, Roumania
[b] "Al. I. Cuza" University, Faculty of Chemistry, 11 Carol I, Iaşi-700506, Roumania
[c] "Al. I. Cuza" University, Research Department, Faculty of Chemistry, 11 Carol I, Iaşi-700506, Roumania

Received November 8, 2016

Metal ion-associated conformational changes of peptides are thought to be the prime mechanism of amyloid formation in several neurodegenerative diseases. The N-terminal, three histidine-containing 16 amino acid residue sequence of amyloid-β peptide (Aβ) is considered the binding site of heavy metal ions. Metal binding to amyloid-β peptides generate oligomers and amyloid plaques associated with Alzheimer's disease (AD) pathology. Since the mechanism of binding metal ions is still elusive and the influence of some other amino acid residues is not clear, we have synthesized five Ala and Gly peptides, with three histidine (His) residues in various positions of their sequences. We thus focus on the peptide properties induced only by the His residues and not by the other amino acids. Then, the electrospray ion trap mass spectrometry (MS), Fourier transform infrared spectroscopy (FT-IR), and circular dichroism spectroscopy (CD) were used to characterize the newly synthesized peptides. The analysis of FT-IR and CD spectra showed that peptide conformation could be related to both peptide composition (e.g. amino acid composition) and sequence specificity of each investigated oligopeptide. In fact, the position of each histidine as well as the other amino acid residues is a key factor of all peptide properties. Only one of the Ala peptides was highly α-helical, whereas the other isomer sequence was less structured. The five peptides are designed for a better understanding of metal ions binding mechanism to His peptides.

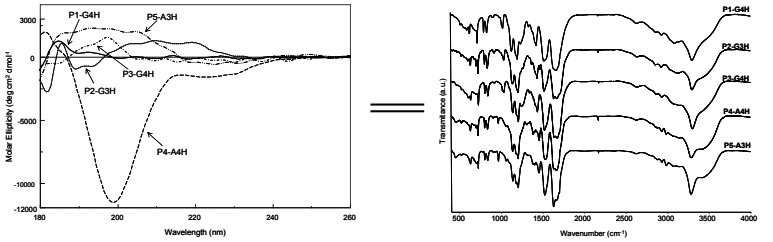

INTRODUCTION

Protein misfolding is at the origin of several neurodegenerative disorders such as Alzheimer, Parkinson and Creutzfeldt–Jacob diseases in humans, and scrapies and spongiform encephalopathies in animals.[1-6] Conformational transitions are thought to be the prime mechanism of amyloid formation in prion diseases.[6-8] The pathogenical conversion of PrP^c into PrP^{Sc} might involve the AGAAAAGA region. Further, AGAAAAGA peptide blocks the toxicity of PrP (106–126), suggesting that this sequence is necessary for the interaction of PrP (106–126) with neurons.[9] The glycine-rich GGGTHSQW sequence in the unstructured amyloidogenic part of the prion protein is a potential pH-dependent binding site for Cu^{2+} ions.[10] On the contrary, alanine-based peptides are known to form helical structures in aqueous solution because of the high helix propensity of alanine.[11,12] The circular dichroism (CD) and Fourier transform infrared (FT-IR) spectroscopic methods have been successfully applied to the conformational studies of alanine-rich peptides in

* Corresponding author: gabidr@uaic.ro

water, methanol and trifluoroethanol.[13-15] Nevertheless, the causes and the mechanisms of the protein misfoldings are not clearly understood yet.[16]

Advanced studies in proteomics field rely on new tools in order to identify and characterize mechanism of protein misfoldings.[17-20] These include spectroscopic methods such as circular dichroism (CD), nuclear magnetic resonance (NMR), Fourier transform infrared (FT-IR) and more recently mass spectrometry (MS) that have been used since decades. Moreover, mass spectrometry has become a crucial instrument for metal-protein interaction[21-24] and protein sequencing.[25] Introduction of electrospray ionization[26] and laser desorbtion ionization[27] contribute to the study of non-covalent interactions in biomolecules. Other studies, in which tetra-glycine[28,29] and histidine containing peptides[30,31] were investigated, revealed that the secondary structure content depends much on the amino acid sequence.

Previously, four histidine-containing oligopeptides were synthesized and some of their metal complexes studied.[32,33] However, their structure-properties relationship has not been thoroughly investigated so far in spite of they are conformationally different one from another, and such properties may induce various patterns of heavy metal binding. Meanwhile, we have synthesized another 19-residue peptide, which is the amide form of the glycine-based peptide with three histidines in the positions 5, 10, and 15 of the glycine backbone. Therefore, the five 19 amino acid sequences consist of alanine or glycine backbones in which these residues in the positions 5, 10, and 15, as well as 4, 8, and 12 have been replaced by histidine.

The goal of this work is to investigate the conformational differences between the five peptides and to examine potential mechanisms based on structure-properties relationship that underlie such differences. These peptides are of paramount interest for investigating the relationship between metal ions and peptides or proteins involved in many degenerative diseases. They were characterized by matrix-assisted laser desorption/ionization time-of-flight mass spectrometry (MALDI-ToF MS), whereas their conformation was investigated by CD and FT-IR spectroscopy. In addition, the properties of the five peptides were theoretically anticipated with the help of GPMAW software.

RESULTS AND DISSCUSION

Peptide synthesis and characterization

The following sequences of peptides were synthesized: 1) H_2N-(Gly-Gly-Gly-Gly-His)$_3$-(Gly)$_4$-COOH (P1-G4H); 2) H_2N-(Gly-Gly-Gly-His)$_3$-(Gly)$_7$-COOH (P2-G3H); 3) H_2N-(Gly-Gly-Gly-Gly-His)$_3$-(Gly)$_4$-$CONH_2$ (P3-G4H); 4) H_2N-(Ala-Ala-Ala-Ala-His)$_3$-(Ala)$_4$-COOH (P4-A4H); and H_2N-(Ala-Ala-Ala-His)$_3$-(Ala)$_7$-COOH (P5-A3H). All five peptides were synthesized as described in the experimental part and purified by RP-HPLC chromatography on a C18 column. Depending on the specific hydrophobicity, each peptide eluted at various elution times. For example, P2-G3H eluted at 13.427 min, being accompanied by some other impurities, which were released (not shown). Thus, the analytical RP-HPLC chromatograms of the five newly synthesized peptides showed major peaks at various minute retention times, because their hydrophobicity varies much with the peptide sequence. Each peak was collected, lyophilized and then analyzed by MALDI-ToF mass spectrometry

MALDI-ToF MS is useful to analyze small proteins and peptides. Besides the signal of the intact molecular ion $[M+H]^+$, at m/z 1342 (P1-G4H and P2-G3H), m/z 1341 (P3-G4H), and m/z 1566 (P4-A4H and P5-A3H), some other two additional peaks, characteristic to Na^+ and K^+ adducts were observed (Fig. 1). Thus, the MALDI-ToF mass spectrum of peptide P1-G4H showed a characteristic signal, which was assigned to the molecular ion $[M+H]^+$ at m/z 1343.4, whereas the characteristic additions of +22 amu and +38 amu to the molecular ion of P1-G4H at m/z 1365.7 and 1381.9 were observed as well, being attributed to sodium and potassium adducts. The signals for the molecular ions of P2-G3H and P3-G4H peptides $[M+H]^+$ were found at m/z 1343.4 and m/z 1342.4, respectively. The MALDI-ToF mass spectrum of peptides P4-A4H and P5-A3H, showed both molecular ions $[M+H]^+$ at m/z 1567.3 and m/z 1567.6, and characteristic signals for $[M+Na]^+$ at m/z 1590.0 together with the signals for y_{17}^{3+} and y_{18}^{3+} and signals for $[M+Na]^+$ at m/z 1588.6 and $[M+K]^+$ at m/z 1605.7.

Theoretical data obtained by using the GPMAW program were in best agreement with the m/z values obtained by MALDI-ToF mass spectrometer for all histidine-containing peptides (Table 1).

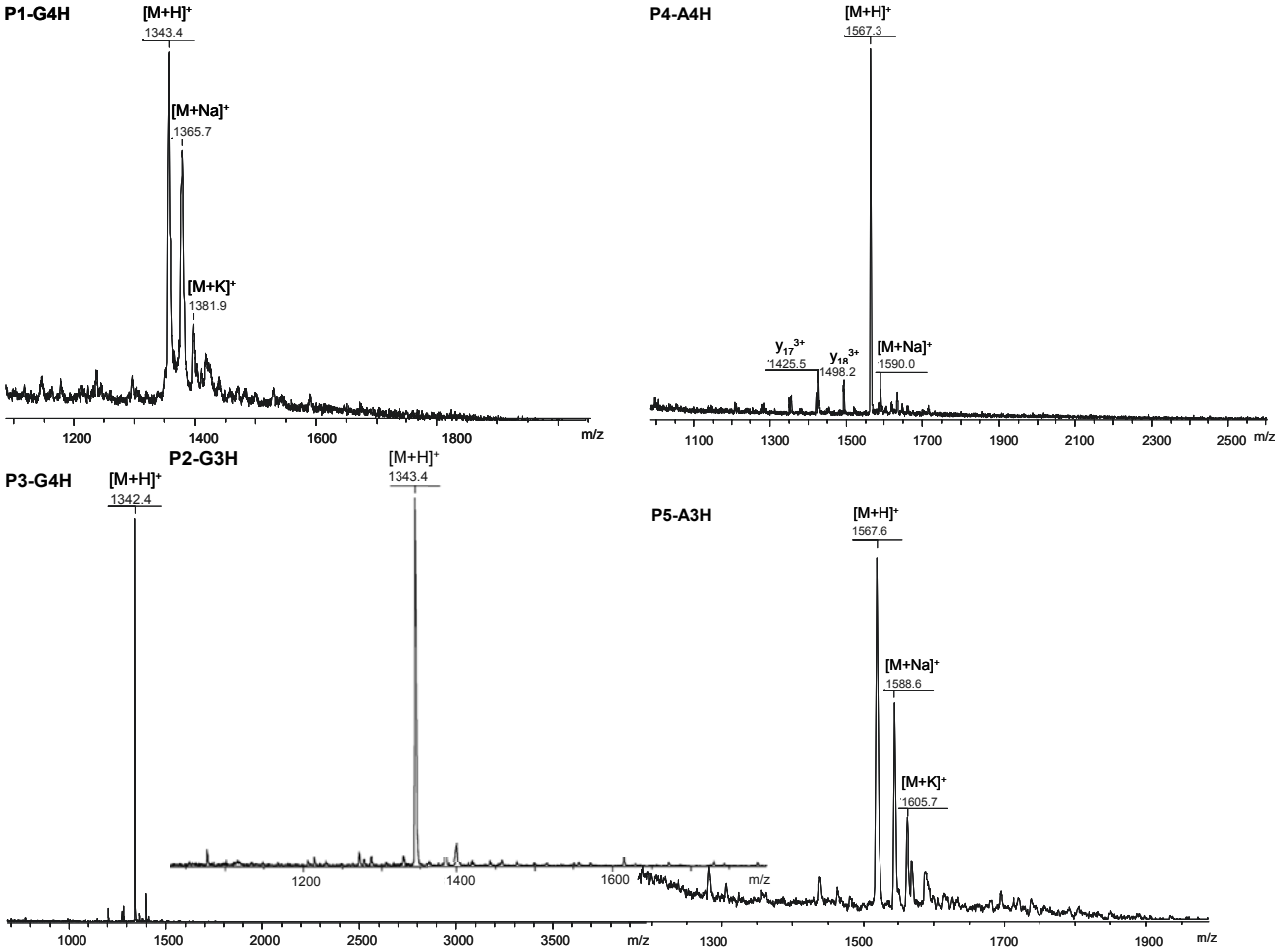

Fig. 1 – MALDI-ToF MS spectra of the newly synthesized histidine-containing peptides: Glycine-based peptides, P1-G4H (-COOH), P2 G3H (-COOH), and P3-G4H (-$CONH_2$), as well as alanine-based peptides, P4-A4H (-COOH) and P5-A3H (-COOH), respectively.

Table 1

Molecular weight of five newly synthesized peptides, as experimentally determined with a MALDI-TOF instrument or calculated with a GPMAW soft

Peptide	Calculated molecular weight, amu		Experimentally found molecular weight, amu
	Monoisotopic	Average	MALDI-TOF MS
P1-G4H	1341.5	1342.3	1342.4
P2-G3H	1341.5	1342.3	1342.4
P3-G4H	1340.6	1341.3	1341.4
P4-A4H	1565.8	1566.7	1566.3
P5-A3H	1565.8	1566.7	1566.6

CD experiments

Circular dichroism (CD) refers to the differential absorption of left- and right-handed circularly polarized light, being used to investigate the secondary structure of peptides and proteins.[34,35] On studying the five His-containing peptides, different conformational patterns were noticed (Fig. 2). For example, glycine-rich peptides, although their backbones are very flexible, seem to be structured and present both high proportion of α-helical conformers and β-turn and random coil forms. We supposed that the presence of β-turn conformers in aqueous solutions of Gly peptide is related to high flexibility induced by glycine residues. Even if alanine is well known for inducing α-helix conformers, P4-A4H had rather disordered molecules, with tendency to form β-sheet conformers. However, P5-A3H peptide displayed high content of α-helical conformers, as the theory claims.[11,12]

Nevertheless, the Gly peptides P1-G4H, P2-G3H and P3-G4H, due to the large number of non-chiral amino acid glycine, gave less structured conformers (Fig. 2; Table 2). Therefore, both negative and positive contributions in CD spectra of the two glycine-rich peptides were very low. However, these peptides had various proportions of α-helical and β-turn conformers, but such conformational proportions are not stable being subjected to the influence of environmental conditions (pH, concentration, type of solvent, temperature). Thus, P1-G4H peptide was found to contain the following proportion of conformers: 51.4% random coil, 21.5% β-turn and 27.1% α-helix (Table 2), as calculated through the spectropolarimeter soft. It was interesting to observe that the helical content of P2-G3H peptide increased up to 78.1%, in spite of the same chemical composition in amino acids and similar proportion of β-turn conformers. Such result was correlated with the presence of seven glycine residues at the carboxylic end of this peptide. The amide form of P1-G4H, the P3-G4H peptide, was characterized by 63.8% helical content, whereas the β-turn conformers were found in proportion of 36.2%. When replaced glycine by alanine, two peptides, P4-A4H and P5-A3H, resulted, which behaved completely different one from another. Contrary to glycine in peptides, alanine induced the formation of very rigid conformations. As expected, the secondary structure of P5-A3H peptide was, indeed, highly α-helical (70.2%), with a proportion of only 29.8% of β-turn conformers. We assumed that the seven alanine residues at P5-A3H peptide C terminal induce such high content of α-helix conformers. However, in spite of high proportion of alanine residues, P4-A4H peptide showed no helical structure. The analysis of P4-A4H peptide CD spectrum showed a mixture of 61.4% random coil conformers, 21.0% β-sheet conformers, and 17.6% β-turn conformers.

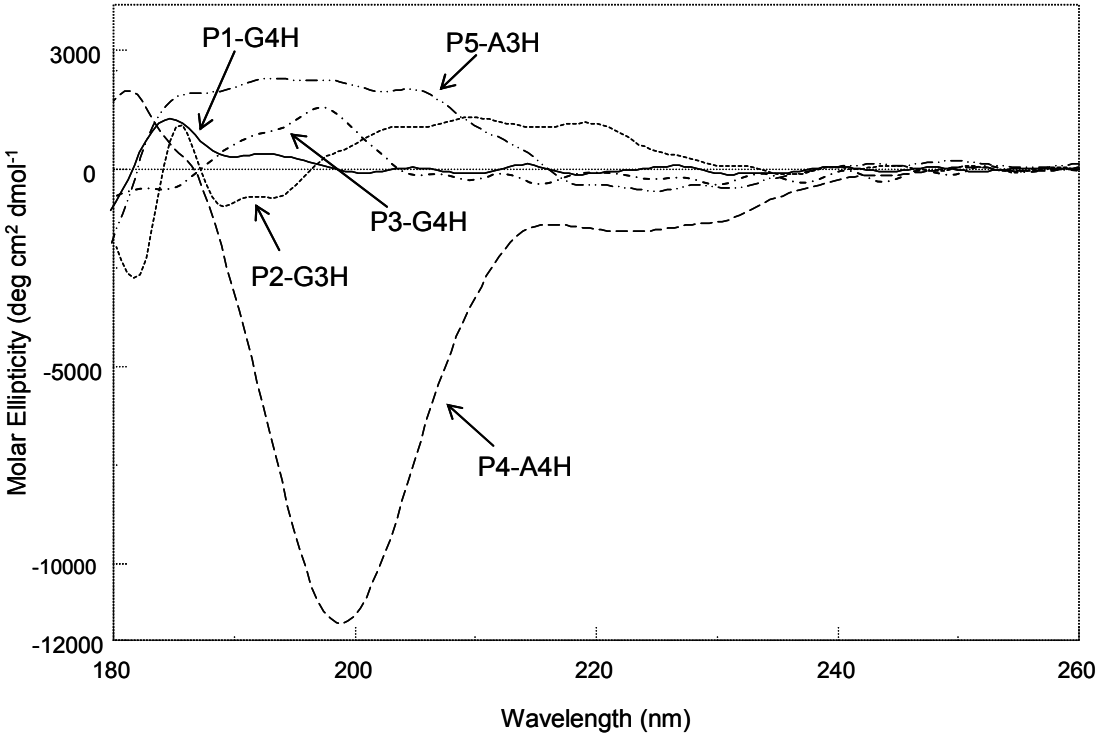

Fig. 2 – Circular dichroism spectra of the five new histidine-containing peptides, showing different conformational patterns due to their sensitivity toward the type of backbones and the position of each histidine residue.

Table 2

Conformational changes of five newly synthesized histidine-containing peptides

Conformation (%)		P1-G4H	P2-G3H	P3-G4H	P4-A4H	P5-A3H
Jasco-715 spectro-polarimeter	α-Helix	27.1	78.1	63.8	0.0	70.2
	β-Sheet	0.0	0.0	0.0	21.0	0.0
	β-Turn	21.5	21.9	36.2	17.6	29.8
	Random coil	51.4	0.0	0.0	61.4	0.0

Table 2 (continued)

GOR method	α-Helix	41.0	39.3	41.0	47.9	50.6
	β-Sheet	11.0	11.9	11.0	16.0	17.1
	β-Turn	21.0	22.8	21.0	24.4	21.6
	Random coil	27.0	26.0	27.0	11.7	10.7

Protein structure prediction is one of the most important tasks of bioinformatics and theoretical chemistry, while the GPMAW soft could be important to understand peptide conformations of interest for medicine (neurodegenerative diseases) and biotechnology. We used GOR method for prediction the secondary structure of the five peptides (Table 2). The GOR information theory-based method was advanced by Garnier, Osguthorpe, and Robson for the prediction of secondary structures in proteins.[36] The GOR method is based on both the propensities of individual amino acids to form particular secondary structures and the conditional probability of the amino acid to form a secondary structure, given that its immediate neighbors have already formed that structure. The GOR estimation resulted in proportion of average 40.4% α-helix conformers in the case of Gly peptides and 49.2% for Ala peptides, whereas the soft installed on the CD instrument estimated the following average values: 56.33% and 35.1%, respectively. Nevertheless, the last proportions seem to estimate better the CD spectral shapes. When calculated the correlation coefficient r, we found a very strong positive correlation between the values obtained from Jasco-715 soft and GOR method for P5-A3H peptide (r = 0.963), followed by those for P2-G3H (r = 0.856). The other Gly peptides, P1-G4H and P3-G4H, were characterized by weaker correlations (r = 0,567 and r = 0.750, respectively). A negative correlation was observed in the case of P4-A4H values (r = – 0.807).

The study of data in Table 2 indicated an unusual behavior of the five peptides as compared with the normal peptides containing one or more amino acid residues. For instance, the amidation of P1-G4H peptide resulted in a more structured α-helical peptide, whereas histidine in the position 5, 10 and 15 in the Ala-based peptides turns α-helix into an unstructured conformer. Such behaviors have not previously been reported.

When studied the effect of environmental conditions on peptide conformation, CD spectra of the peptide P1-G4H proved to be dependent on pH, the type of solvent and the presence of salts, such as ammonium acetate (Fig. 3). Under aqueous conditions, at pH below 7.00, the P1-G4H free peptide had 27.1% α-helix conformers and 21.5% β-turn ones (Table 2). Generally, trifluoroethanol (TFE) solutions induce peptides to form α-helical structures in aqueous solutions. Although the CD spectrum in TFE was found different from that in water, the proportion of α-helix P1-G4H molecules decreased much.

However, TFE is known to preferentially stabilize peptides in ordered conformation (α-helix). Nevertheless, P1-G4H molecules were found rather as β-turn structures in TFE, and not α-helical conformers. The conformation of P1-G4H also changed much when pH rose from 7.4 to pH 8.5: the proportion of α-helix conformers decreased to 9.3%, and that of β-turn forms increased dramatically (90.7%). At pH 7.4, the content of α-helical forms was very low, while β-turn proportion was found to be 55.7%. Moreover, the peptide molecules became more structured (random coil proportion decreased from 51.4% to 44.3% in pH 7.4 aqueous solution).

Only one or two ππ* and one or two *n*π* amide transitions have been used in peptide CD calculations.[37] The –CONH- group contains four π electrons, three π orbitals (π_+, π_o and π*) and two lone pairs of electrons in the non-bonding orbitals (*n* and *n'*) of the valence shell. Thus, two ππ* transitions ($\pi_o \rightarrow \pi^*$ seen at 190 nm, electric dipole transition moment, $\mu \approx 3.1$ Debyes, D; and $\pi_+ \rightarrow \pi^*$ seen at 139 nm, $\mu \approx 1.8$ D), and one *n*π* (*n*→π*, 220 nm) transition in the amide chromophore have been identified. The α-helical CD spectrum has two negative bands at 222 nm and 208 nm, and a positive band at 192 nm (Fig. 2).

The β-turn secondary structure is formed by three residues and stabilized by a hydrogen bond between the first and the third amide group, which effectively reverses the direction of chain propagation. β-Sheet spectrum has a negative band near 215 nm (n→π*) and a positive band near 195-198 nm (π→π*). From Fig. 2 and Table 2, a close correlation between absorption bands and the proportions of the corresponding conformers was noticed.

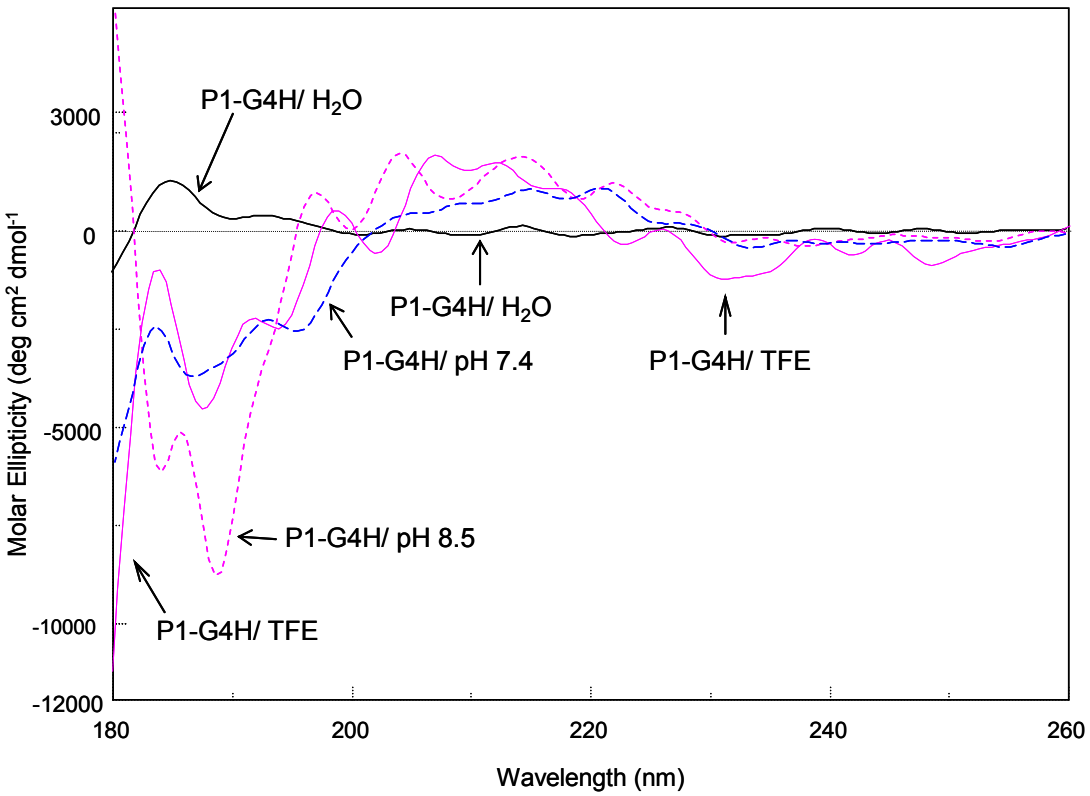

Fig. 3 – Circular dichroism spectra for 200 μM solutions of P1-G4H peptide under various environmental conditions: 200 μM aqueous solution (P1-G4H/ H_2O); 50% trifluoroethanol solution (P1-G4H/ TFE); ammonium acetate pH 7.4 buffer (P1-G4H/ pH 7.4); and ammonium acetate pH 8.5 buffer (P1-G4H/ pH 8.5).

FT-IR Study

The infrared spectra of the five newly synthesized peptides were also found dissimilar. However, some peaks were similar, whereas some more others had different shapes or intensities (Fig. 4). The five peptides had a characteristic signal at 722 cm^{-1}, which was assigned to C-H bond. Identical signals were also found at 628 cm^{-1} (assigned to C-H vibration in the imidazole ring of histidine), 799 cm^{-1}, 855 cm^{-1}, 1135 cm^{-1}, and 1202 cm^{-1} (assigned to C-N bond), respectively. The signal at 855 cm^{-1} is also a characteristic of the aromatic moiety of histidine. The 1202 cm^{-1} was assigned to the vibration of C-N amine group, existed at N-terminal end of each peptide. However, several signals differentiated Gly-peptides (P1-G4H, P2-G3H and P3-G4H) from Ala peptide (P4-G4H and P5-G3H). For example, the latter ones displayed a very characteristic signal at 965 cm^{-1}, whereas Gly peptides showed a peak, which was shifted toward 1028-1030 cm^{-1}. We compared the spectra of the newly synthesized peptides with that of imidazole ring and found the signal around 1450 cm^{-1} was shifted toward 1432 cm^{-1} in Gly peptides.

In the spectrum of peptides P4-G4H and P5-G3H this signal was found at 1454 cm^{-1}. Imidazole moiety also gives a characteristic peak around 1050 cm^{-1}, which was found in Gly peptides at about 1028-1030 cm^{-1} and at 1055 cm^{-1} in the case of Ala peptides P4-G4H and P5-G3H. The methyl groups in Ala residues of P4-G4H and P5-G3H were identified with C-H absorption at 1380 cm^{-1}. Intense signals of imidazole at 2850 cm^{-1} and 2930 cm^{-1} were found also in the spectra of all peptides, although they were shifted toward 2878 cm^{-1} and 2936 cm^{-1} in the case of P4-G4H and P5-G3H. All together, the shapes of the five peptides differ much one from the others. Even P1-G4H and P3-G4H were found to differ one from another (the Amide I band at 1600-1700 cm^{-1} is an example).

The absorption band at around 3300 cm^{-1} was intense, and was assigned to N-H absorption ($\nu_{N\text{-}H\ sim}$ and $\nu_{N\text{-}H\ asim}$). Although it seems to be similar in all spectra, the maximum of absorption was found at various wave number values (P1-G4H – 3315 cm^{-1}; P2-G3H - 3298 cm^{-1}; P3-G4H - 3299 cm^{-1}; P4-A4H - 3289 cm^{-1}; P5-A3H - 3284 cm^{-1}). Besides, the shoulder seen near these bands were more prominent in the case of Ala peptides. Such data were explained by the existence of various secondary structures of these peptides which allow different interactions between NH_2 group and the other ones such as -COOH or –CONH- groups.

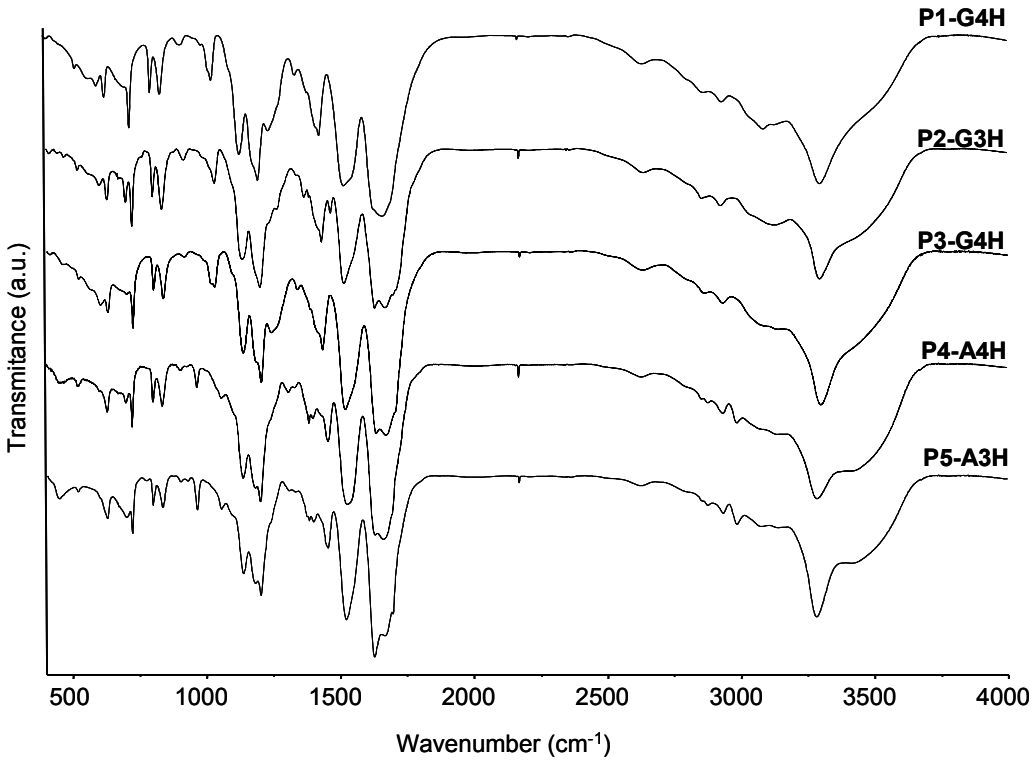

Fig. 4 – FT-IR spectra of the newly synthesized histidine-containing peptides.

Moreover, a large but less intense band was found in the range from 3342 to 3470 cm^{-1}, which was associated with the formation of hydrogen bonds. In the case of Ala peptides, this absorption band was more intense, probably due to the formation of more hydrogen bonds which stabilize the secondary structure.[15,38]

The analysis of FT-IR spectra can therefore provide information on both the structure and inter- and intramolecular interactions. The peptide group afforded more characteristic bands which do represent different vibrations of the protein moiety. The amide A band (about 3500 cm^{-1}) and amide B (P1-G4H - 3090 cm^{-1}, P5-A3H – 3074 cm^{-1}, etc.) originate from a Fermi resonance between the first overtone of amide II and the N—H stretching vibration. These modes of vibration do not depend on the backbone conformation but are very sensitive to the strength of a hydrogen bond for hydrogen bond lengths between 2.69 to 2.85 Å.[39]

Amide I and II bands of peptides in the infrared spectrum are sensitive to their conformation. The amide I band (between 1600 and 1700 cm^{-1}) was the most intense absorbance band for all the five peptides and mainly associated with the C=O stretching vibration. It is directly related to the backbone conformation. This band had a characteristic shape for each peptide investigated. For example, P1-G4H displayed a large band in the range from 1632 cm^{-1} to 1680 cm^{-1}, with the maximum of absorption at 1667 cm^{-1}. P2-G3H showed two peaks in the band area, at 1631 cm^{-1}, and 1681 cm^{-1}, respectively. This band was larger than that of P1-G4H, in the range from 1628 cm^{-1} to 1683 cm^{-1}. Indeed, the secondary structures of the two peptides, P1-G4H and P2-G3H, were found to be different, as shown in Fig. 2. P3-G4H has presented a shape of the absorption band close related to that of P2-G3H. P3-G4H had a large band in the range from 1632 cm^{-1} to 1686 cm^{-1}. The shift toward higher wave numbers might represent the contribution by $CONH_2$ group. P4-A4H and P5-A3H displayed different absorption bands related to the peptide groups. P4-A4H had a low absorption peak at a wave number around 1630 cm^{-1}, and an intense absorption at 1674 cm^{-1}, whereas P5-A3H was characterized by a more intense one at about 1629 cm^{-1} (between 1626 cm^{-1} and 1631 cm^{-1}), and a weaker one at about 1667 cm^{-1}).

Amide II band is related to the N—H bending vibration and the C—N stretching vibration (18-40%). The investigated peptides showed various amide II bands (P1-G4H displayed an intense band at 1524 cm^{-1}, P2-G3H – 1516 cm^{-1}, P3-G4H – 1518 cm^{-1}, P4-A4H – 1529 cm^{-1}, and P5-A3H – 1523 cm^{-1}). Since the amide I absorption is primarily determined by the backbone conformation and independent of the amino acid

sequence, its hydrophilic or hydrophobic properties and charge, we analyzed the conformational properties of these peptides. Some amino acid residues favor the formation of extremely strong intermolecular hydrogen bonds, resulting in an intense amide I feature at 1610 to 1628 cm^{-1} for denatured, aggregated peptides. P5-A3H might thus form aggregated strands that appear in FT-IR spectrum at 1626 to 1631 cm^{-1}. However, β-sheet structure may appear in the same range from 1625 to 1640 cm^{-1}. Nevertheless, the band at 1630-1648 cm^{-1} has to be assigned to 3_{10}-helices rather than β-structure.[40] These results are concordant with the physico-chemical properties of P5-A3H peptide which is readily aggregating.

Denaturized or unfolded proteins with the most extended peptide chains should display the lowest amide I frequencies, because the intra-molecular hydrogen bonds are impossible. Thus, P2-G3H with its additional absorption band at 1671 to 1683 cm^{-1} could be a candidate to form antiparallel β-sheet aggregated strands (normally at 1675-1695 cm^{-1}). Gly peptides appear to contain high proportion of antiparallel β-sheet aggregates as well as unordered conformers. Although P4-A4H and P5-A3H have the same residues in the sequence, they presented different proportions of ordered and unordered conformers, P5-A3H being richer in α-helix structures.

Nevertheless for a small number of mainly α-helical proteins the major amide I component is shifted to somewhat lower wave numbers of below 1650 cm^{-1} due to strong solvent-protein interactions or distortion of structural elements.[38] In this case, the proportion of α-helix of these peptide might be much increased.

The COOH group was found at about 2935 cm^{-1} and at 3300 to 3500 cm^{-1} in the spectrum, although its bands interfere with those of C-H bond and hydrogen bond, respectively.

Other signals were assigned to NH_3^+ torsional oscillation (518 cm^{-1}), the COO^- out of plane bending (600 cm^{-1}), COO^- bending (698 cm^{-1}), and C-H stretch (721 cm^{-1} and 2926-2936 cm^{-1}). Absorption band of medium intensity at 2637 cm^{-1} is due to N-H…O bond.

GPMAW study

Not only peptide masses, but also HPLC elution times, charge versus pH, MS/MS fragmentation, *etc.*, can be obtained from the computer program GPMAW. Fig. 5 shows the hydrophobicity index of the five peptides as calculated by the GPMAW soft. Similar indices were calculated for both P1-G4H and P3-G4H indicating that the $–CONH_2$ group has no influence on the hydrophobic character of peptides. In spite of the same composition, P1-G4H had different hydrophobicity from that of P2-G3H, due to the position of the three histidines and the seven terminal glycine residues. Furthermore, the Ala peptides differ one from another, whereas the seven carboxyl terminal alanines increased much the hydrophobic properties of this molecule end.

As for the isoelectric point, pI, GPMAW software afforded the calculated charges versus pH, where pI for all five peptides varied between pH 7.64 and pH 7.71, due to the three histidine in each sequence, which induce rather alkaline properties of host peptides (P1-G4H – pH 7.67; P2-G3H – pH 7.64; P3-G4H – pH 7.66; P4-A4H – pH 7.70; P5-A3H – pH 7.71).

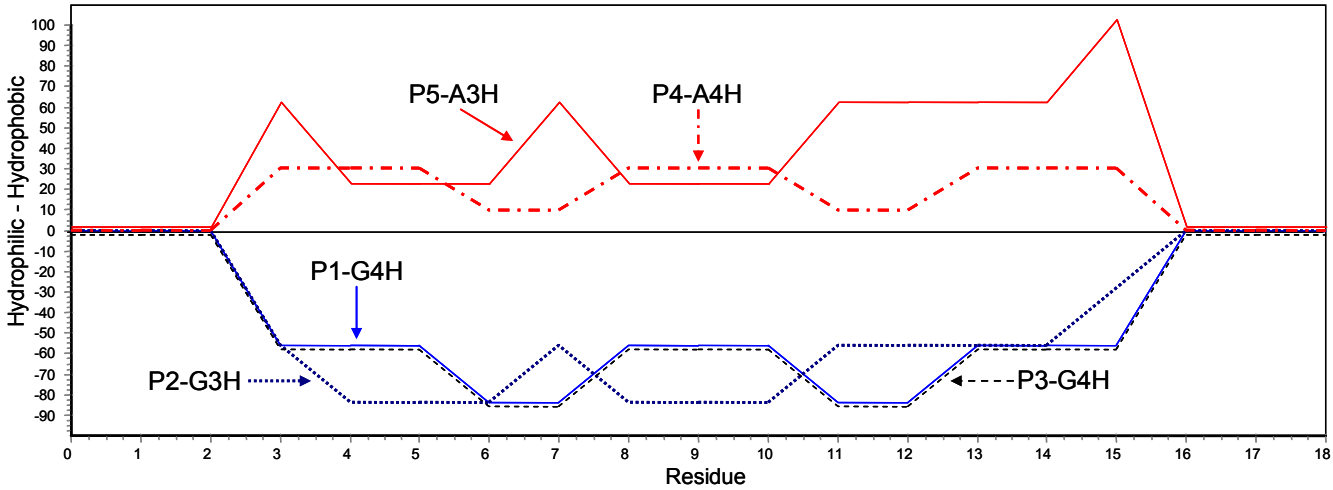

Fig. 5 – Hydrophobicity index for the five peptides as calculated by the GPMAW soft.

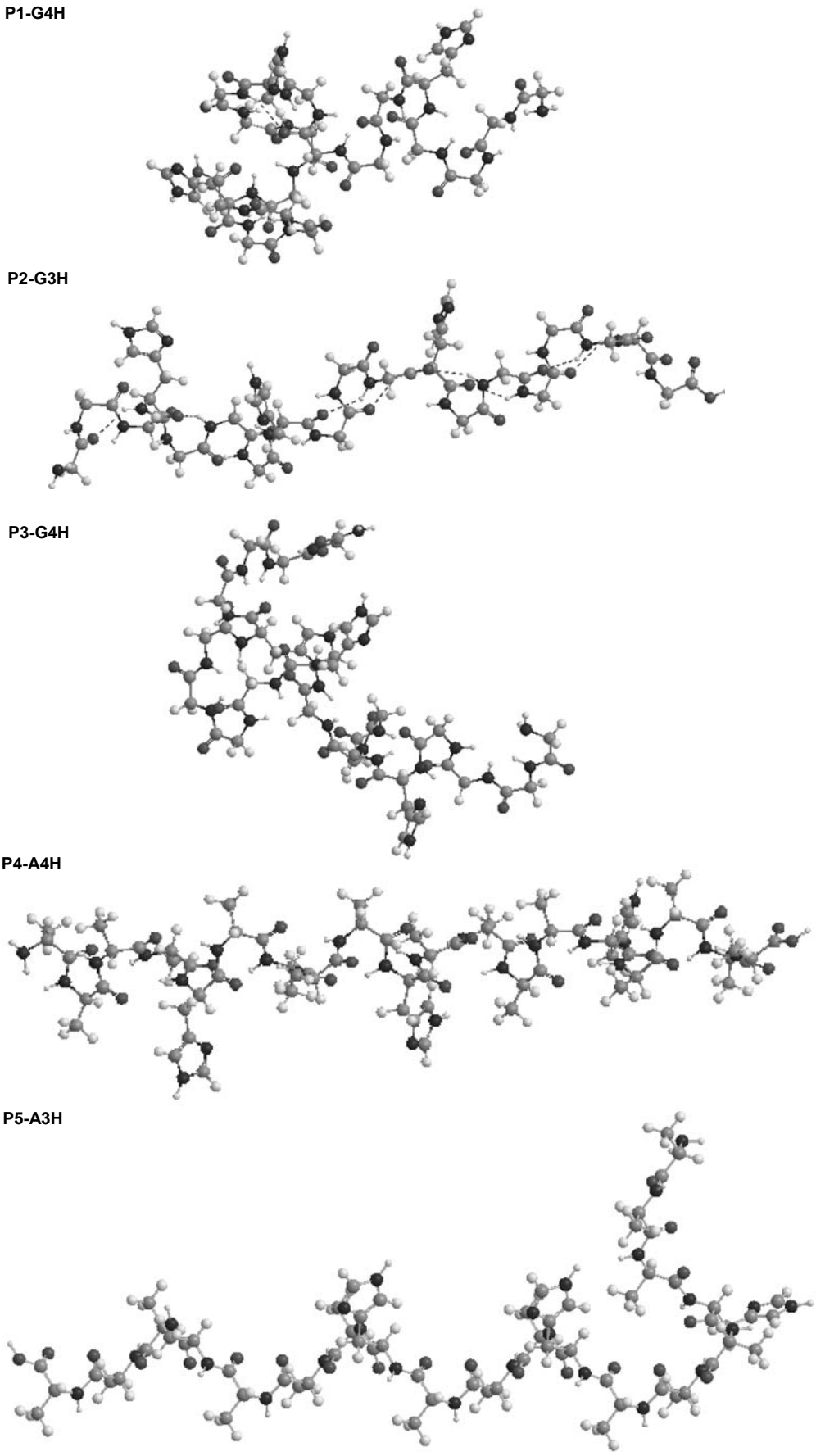

Fig. 6 – Possible spatial structures of the newly synthesized peptides.

Biomedical implications

It is known that amyloidal peptides form dimmers and oligomers that are very noxious in cell culture experiments, and that aggregation is causative of the neurodegeneration seen in AD. The transformation of the unordered molecules into the β-sheet conformers determines the self-aggregation and the fibril formation.

The alanine-rich palindromic sequence of human PrP (amino acid residues 113 to 120: AGAAAAGA) has also been shown to be important in the conversion of PrPC to PrPSc, associated with prion diseases.[41] Therefore, both Ala and Gly synthetic peptides do represent model molecules for understanding the conformational changes of amyloid peptides associated with the neurodegenerative pathologies. Moreover, histidine is involved in binding heavy metal ions. Further research should be undertaken in order to demonstrate how the newly synthesized peptides bind heavy metal and how their conformation is changing during such process.

Spatial structure of peptides

Using Chem3D Ultra 10.0 software, we calculated arrangement in space, energy and chemical bonds distances to find possible structures of the complexes (Fig. 6). Our computer simulation studies clearly showed that both Gly peptides and Ala peptides are different one from another. However, P1-G4H and P3-G4H seem to be similar in shape and both are different from P2-G3H. P5-A3H peptide is clearly α-helical.

EXPERIMENTAL

Materials

NovaSyn TGR and TGA resins as well as Wang resin with preloaded glycine were purchased from NovaBiochem (Fig. 7). Protected amino acids for peptide synthesis were provided by GL Biochem (Shanghai, China). All solvents for peptide synthesis were commercially analytical grade and were redistilled before use. Dimethylformamide (DMF), piperidine, 4-methylmorpholine were purchased from Sigma Aldrich (St Louis, MO, SUA) and bromophenol blue, ninhydrin, acetonitrile, trifluoroethanol (TFE), and trifluoroacetic acid (TFA) were from Merck. All chemicals were of analytical reagent grade and all solutions were prepared in MilliQ grade water with R = 18.2 MΩ·cm.

Instruments

Some histidine-containing peptides were synthesized by using ResPep SL automated peptide synthesizer (Intavis, Germany). Some other peptides were manually synthesized. For peptide purification, a BIO-RAD Model 2700Elite RP-HPLC system (Bio-Rad Laboratories GmbH, Germany) using Spherisorb (ODS) C_{18} and C_8 semi-preparative columns was used. MALDI-TOF MS analysis was carried out with a Bruker Biflex linear TOF mass spectrometer equipped with a nitrogen UV laser (λ_{max} 337 nm) and a delayed extraction system, a dual channel plate detector, a 26-sample SCOUT source, a video system and a XMASS data system for spectra acquisition and instrument control. CD spectra were recorded using a Jasco-715 spectropolarimeter (Labor and Datentechnik GmbH, Germany). FT-IR spectra were recorded with a Shimadzu Model 8400S spectrophotometer.

Synthesis of oligopeptide

The following five peptides (100 μM) were synthesized: H_2N-GGGGHGGGGHGGGGHGGGG-COOH (P1-G4H), H_2N-GGGHGGGHGGGHGGGGGGG-COOH (P2-G3H), H_2N-GGGGHGGGGHGGGGHGGGG-$CONH_2$ (P3-G4H), AAAAHAAAAHAAAAHAAAA-COOH (P4-A4H), and AAAHAAAHAAAHAAAAAAA-COOH (P5-A3H), respectively (where A is alanine, G is glycine and H is histidine). The peptides P1-G4H and P2-G3H were automatically synthesized with a ResPep synthesizer on Fmoc-Gly-Wang resin (Fig. 7a); the C-terminal end-amidated P3-G4H peptide was automatically prepared on a TGR resin. NovaSyn® TGR resin is prepared from NovaSyn® TG amino resin by derivatization with the modified Rink linker (Fig. 7c), which is designed to release peptide amides upon the final cleavage. A pre-defined protocol and ready-to-use amino acid cartridges of the ResPep synthesizer were used. To assembled peptides, the ResPep activated dry amino acids, and the solutions to the resin support delivered in a synthesis column. The final result was a support carrying the desired peptide of choice, which was then cleaved off manually.

The peptides P4-A4H and P5-A3H were manually synthesized on a TGA resin as solid supports (Fig. 7b), as previously described.[42] All 19-residue peptides with high capacity of binding metal cations due to the presence of histidine residues were prepared by the classical Merrifield Fmoc methodology, which is more robust and environmentally safe.

The two peptides, P4-A4H and P5-A3H, were prepared manually in a glass reaction vessel (30 mL) fritted with a sintered glass frit. Side chain protecting groups included trityl (Trt) for His. Solvent and soluble reagents were removed by suction. Washings of resin were performed with dichloromethane (DCM), ethanol (EtOH) and DMF (each with 5 mL, 3 × 2 min). The Fmoc-amino-acids, Fmoc-Ala-OH, Fmoc-Gly-OH, and Fmoc-His(Trt)-OH were attached to the resin one by one using N-methylmorpholine as the coupling reagent.

Following Fmoc-Ala-OH or Fmoc-Gly-OH preactivation using PyBOP (benzotriazol-1-yl-N-oxytripyrrolidinophosphonium hexafluorophosphate), 100 μL of N-methylmorpholine dissolved in the smallest amount of DMF and poured into the resin. The coupling reaction mixture was maintained at room temperature for one hour, being verified by the ninhydrin (Kaiser) test. The double coupling process was performed under the same conditions when the ninhydrin test was positive. After washing the resin, the Fmoc group was removed by piperidine/DMF (20%) as above-mentioned. Afterwards, the coupling procedures of the other Fmoc-amino acids were similarly performed.

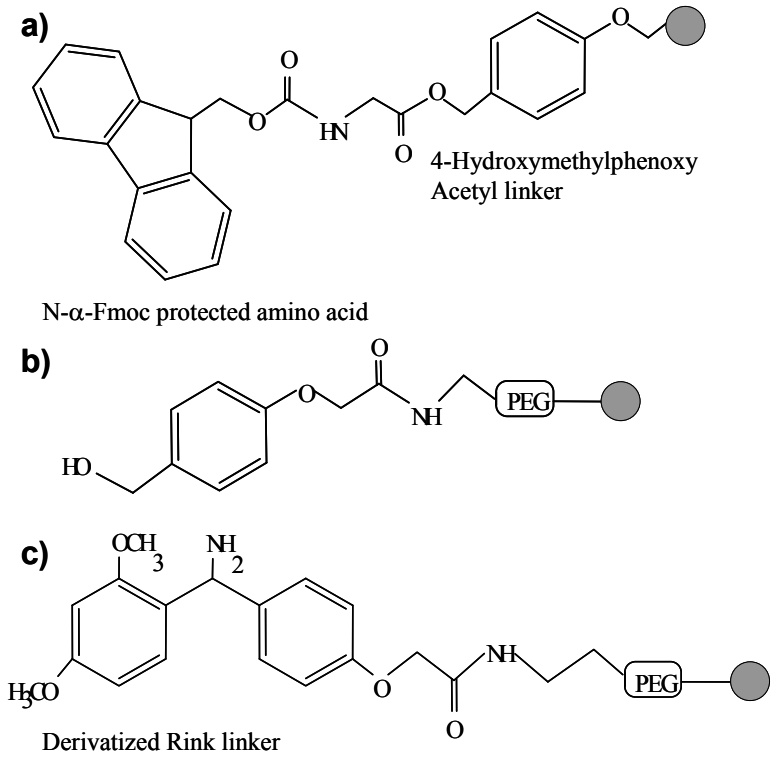

Fig. 7 – Schematic representation of resins used for peptide synthesis:
a) Fmoc-Gly-Wang resin; b) NovaSyn® TGA resin; c) NovaSyn® TGR resin.

After the final step of deprotection of Fmoc group, the obtained resin-bound peptide was dried in vacuum and treated with trifluoroacetic acid (TFA)/H_2O/triethylsilane (TES) (90/5/5, v/v, 4.5 mL TFA/0.25 mL H_2O/0.25 mL TES,) for 3 hours to cleave the peptide from the resin and remove the side chain protecting groups. After cleavage from the resin, the peptides were precipitated with *t*-butyl methyl-ether, washed with diethyl ether and dissolved in 5% acetic acid prior to freeze-drying. Crude products were characterized by analytical RP-HPLC and MALDI-ToF and if necessary purified by semipreparative RP-HPLC.

Chromatography

The peptides (1 mg) were dissolved in 1 mL of acetonitrile/water (80:20, v/v containing 0.1% TFA), filtered and manually injected through an injector with 10 μL sample loop. The mobile phase used consisted in: A: 0.1% aqueous TFA and B: 0.1% TFA in acetonitrile-water (4/1, v/v), with a flow-rate of 4 mL/min. 5% B and 95% A were used in the first 5 min, and a linear gradient of 5 to 45% B over the next 40 min. Eluted products were detected at 220 nm.

MALDI-ToF mass spectrometry

For MALDI-ToF MS analysis of peptides, samples were cocrystallized with an excess of organic matrix that absorbs at 337 nm. α-Cyano-4-hydroxy-cinnamic acid (HCCA) was the preferred matrix for peptide mapping. Following a short laser pulse (3 ns), analytes were desorbed and ionized into the gas phase, and their m/z values were determined in a ToF mass analyzer. In ToF analyzers the mass-to-charge ratio of an ion is determined by measuring their flight time. Due to their mass-dependent velocities, ions are separated during their flight. A detector at the end of the flight tube will produce a signal for each ion species. Typical flight times are between a few microseconds and several 100 μs. Mass determination accuracy vary from 0.01% to 0.1% depending on the sample preparation technique and the method of choice for calibration. Results were expressed as atomic mass units (amu or Da).

For measurement, 0.7 μL of freshly prepared matrix solution and 0.7 μL of sample solution were mixed on the stainless steel MALDI target and allowed to dry. Acquisition of spectra was carried out at an acceleration voltage of 20 kV and a detector voltage of 1.5 kV. Fifty to 200 single shots were accumulated into a final mass spectrum. External calibration was carried out using the average masses of singly protonated ion signals of bovine insulin (m/z 5734.5), bovine insulin B-chain, oxidized (m/z 3496.9), bee venom melitin (m/z 2847.5), human adrenocorticotropic hormone (ACTH) fragment (m/z 2466.7), human neurotensin (m/z 1673.9), human angiotensin I (m/z 1297.5), human bradykinin (m/z 1061.2), and human angiotensin II (m/z 1047.2).

CD spectropolarimetry

The measurements were performed in quartz cells with a path length of 0.5 mm, in the range from 180 to 260 nm. For measurements, the following parameters were used: resolution 0.5 nm, band width 1.0 nm, sensitivity 50 mdeg, the response 8 s at speed of 20 nm/min. The peptides were dissolved in ammonium bicarbonate, pH 7.4, at a concentration of 200 μM. For each peptide was recorded six different scans, and baseline spectra were subtracted from each spectrum. All measurements were carried out at 25º C. The direct CD measurements were expressed in molar ellipticity Δε ($M^{-1} \cdot cm^{-1}$), and recalculated as deg cm^2 $dmole^{-1}$.

FT-IR spectroscopy

The FTIR spectra of the peptides were recorded in solid state (KBr), in the frequency region 400–4.000 cm^{-1} under a resolution of 2 cm^{-1} and with a scanning speed of 2 mm/sec. Typically, 200 scans were signal-averaged for a single spectrum and the collected FT-IR spectra were compared with the standard spectra of the functional groups.

Computer software

For the correct molecular weight determination of peptides and the prediction of various fragments obtained in the MS/MS process, a soft named General Protein/Mass Analysis for Window (GPMAW, Lighthouse Data, Denmark) was used. Computer simulation was done with the help of the Chem3D Ultra 10.0 program.

CONCLUSIONS

Five alanine- and glycine-based peptides, containing three histidine residues in various positions, have been synthesized, being designated to serve as models in the investigation of metal binding and the conformational changes of abnormal peptides associated with various neurodegenerative pathologies. The analysis of CD spectra of the peptide revealed that the secondary structure content depends on the peptide composition, the position of each amino acid in the sequence, type of solvent, and pH of the solution at the same concentration. Although alanine induces the formation of α-helical conformers, only the peptide ended with seven alanines was proved to be rich in α-helix populations. While Ala peptides were rather rigid structures, the Gly peptides proved to be very flexible, and their conformation obeys important changes depending on the environmental conditions. The infrared spectra also confirmed the chemical composition and secondary structure of the five peptide molecules. Furthermore, the molecular modeling studies supported the structural changes observed by FT-IR and CD spectroscopy.

Acknowledgements: The authors are indebted to Dr. Marilena Manea and Prof. Dr. Przybylski from Uni-Konstanz for their technical support and advises. Funding from the Roumanian Government within the IDEI Program coordinated by UEFISCDI Bucharest (Contract 313/2011) is gratefully acknowledged. Dr. B. A. Petre acknowledges Project PN-II-RU-TE-2014-4-0920.

REFERENCES

1. J. Brettschneider, K. Del Tredici, V. M. Y. Lee and J. Q. Trojanowski, *Nat. Rev. Neurosci.*, **2015**, *16*, 109-120.
2. B. M. Coleman and A. F. Hill, *Semin. Cell Dev. Bio*., **2015**, *40*, 89-96.
3. R. Morales, L.D. Estrada, R. Diaz-Espinoza, D. Morales-Scheihing, M.C. Jara, J. Castilla and C.J. Soto, *Neurosci.*, **2010**, *30*, 4528-4535.
4. Y. Roettger, Y. Du, M. Bacher, I. Zerr, R. Dodel and J.P. Bach, *Nat. Rev. Neurol.*, **2013**, *9*, 98-105.
5. C. Hureau, C. Mathé, P. Faller, T. A. Mattioli and P. Dorlet, *J. Biol. Inorg. Chem*., **2008**, *13*, 1055–1064.
6. K. S. Satheeshkumar and R. Jayakumar, *Biophys. J*., **2003**, *85*, 473-483.
7. F. A. Aprile, P. Sormanni and M. A. Vendruscolo, *Biochemistry*, **2015**, *54*, 5103-5112.
8. L. G. Rizzi and S. Auer, *J. Phys. Chem. B.*, **2015**, *119*, 14631-14636.
9. D. R. Brown, *Mol. Cell Neurosci*., **2000**, *15*, 66-78.
10. C. Hureau, L. Charlet, P. Dorlet, F. Gonnet, L. Spadini, E. Anxolabéhère-Mallart and J.J. Girerd, *J. Biol. Inorg. Chem*., **2006**, *11*, 735-744.
11. M. Vanhalle, S. Corneillie, M. Smet, P. Van Puyvelde and B. Goderis, *Biomacromolecules*, **2016**, *17*, 183-91.
12. E. A. Gooding, A. Pozo Ramajo, J. W. Wang, C. Palmer, E. Fouts and M. Volk, *Chem. Commun*., **2005**, 5985–5987.
13. M. Rabe, H. R. Zope and A. Kros, L*angmuir*, **2015**, *31*, 9953-9964.
14. S. Anantharaj and M. Jayakannan, *Biomacromolecules*, **2015**, *16*, 1009-1020.
15. K. Bagińska, J. Makowska, W. Wiczk, F. Kasprzykowski and L. Chmurzyński, *J. Pept. Sci*., **2008***, 14*, 283-289.
16. C. Soto and L. D. Estrada, *Arch. Neurol.*, **2008**, *65*, 184-189.
17. N. D. Udeshi, P. D. Compton, J. Shabanowitz, D. F. Hunt and K. L. Rose, *Nat. Prot.,* **2008**, *3*, 1709 – 1717.
18. A. Adochitei and G. Drochioiu, *Rev. Roum. Chim*., **2011**, *56*(7), 783-791.
19. G. Drochioiu, E. N. Damoc and M. Przybylski, T*alanta*, 2006, **69**, 556-564.
20. G. Drochioiu, M. Murariu, I. Mangalagiu and I. Druta, *Talanta*, **2002**, *56*, 425 – 433.
21. G. Drochioiu, M. Manea, M. Dragusanu, M. Murariu, E. S. Dragan, B. A. Petre, G. Mezo and M. Przybylski, *Biophys. Chem.,* **2009**, *144*, 9-20.
22. M. Murariu, E. S. Dragan and G. Drochioiu, *Biomacromolecules*, **2007**, *8*, 3836-3841.
23. R. Gradinaru, M. Murariu, E. Dragan and G. Drochioiu, *Rom Biotech Lett.,* **2007**, *12*, 3235.
24. G. Schlosser, R. Stefanescu, M. Przybylski, M. Murariu, F. Hudecz and G. Drochioiu, *Eur. J. Mass Spectrom.,* **2007**, *13*, 331-338.
25. D. L. Swaney, G. C. McAlister and J. J. Coon, *Nature Methods*, **2008**, *5*, 959-964.
26. J. B. Fenn, M. Mann, C. K. Meng, S. F. Wong and C. M. Whitehouse, *Science*, **1989**, *246*, 64-71.
27. K. Tanaka, H. Waki, Y. Ido, S. Akita, Y. Yoshida, T. Yoshida and T. Matsuo, *Rapid Commun. Mass Sp*., **1988**, *2*, 151-153.
28. L. Ion, C. I. Ciobanu, M. Murariu, V. R. Gradinaru and G. Drochioiu, *Int. J. Pept. Res. Ther.,* **2015**, 1-11.
29. M. Murariu, *Int. J. Mass Spectrom*., **2013**, *351*, 12– 22.
30. M. Murariu, E. S. Dragan and G. Drochioiu, *Biopolymers*, **2010**, *93*, 497-508.
31. M. Murariu, E. S. Dragan and G. Drochioiu, *Int. J. Pept. Res. Ther.,* **2009**, *15*, 303-311.

32. M. Murariu, E. S. Dragan and G. Drochioiu, E*ur. J. Mass Spectrom*., **2010**, *16(4),* 511-521.
33. M. Murariu, E. S. Dragan, A. Adochitei, G. Zbancioc and G. Drochioiu, *J. Pept. Sci*., **2011**, *17*, 512-519.
34. P. Atkins and J. De Paula, "Elements of physical chemistry", Oxford University Press, 2013.
35. N. Berova and K. Nakanishi, "Circular dichroism: principles and applications", John Wiley & Sons, 2000.
36. J. Garnier, J. F. Gibrat and B. Robson, *Methods Enzymol.,* 1996, 266, 540-553.
37. N. Sreerama and R. W. Woody, *Methods Enzymol.,* **2004**, *383*, 318-351
38. M. Jackson and H. H. Mantsch, *Crit. Rev. Biochem. Mol. Biol*., **1995**, *30*, 95–120.
39. S. Krimm and J. Bandekar, *Adv. Protein Chem.*, **1986**, *38*, 181–364.
40. H. Torii and M. Tasumi, *J. Chem. Phys*., **1992**, *96*, 3379–87.
41. B. M. Coleman, C. F. Harrison, B. Guo, C. L. Masters, K. J. Barnham, V. A. Lawson and A. F. Hill, *J. Virol.,* **2014**, *88*, 2690-2703.
42. I. Coin, R. Dölling, E. Krause, M. Bienert, M. Beyermann, C. D. Sferdean and L. A. Carpino, *J. Org. Chem.,* **2006**, *71*, 6171-6177.